

## Domain wall orientation and domain shape in $\text{KTiOPO}_4$ crystals

V. Ya. Shur<sup>\*</sup>, E. M. Vaskina, E. V. Pelegova, M. A. Chuvakova, A. R. Akhmatkhanov, O. V. Kizko, M. Ivanov, and A. L. Kholkin

Citation: *Appl. Phys. Lett.* **109**, 132901 (2016); doi: 10.1063/1.4963781

View online: <http://dx.doi.org/10.1063/1.4963781>

View Table of Contents: <http://aip.scitation.org/toc/apl/109/13>

Published by the [American Institute of Physics](#)

---

### Articles you may be interested in

[Structural and morphological modifications of polymer thin film in the presence of nonsolvent](#)

*Appl. Phys. Lett.* **1731**, 080031080031 (2016); 10.1063/1.4947909

[Intrinsic defect-mediated conduction and resistive switching in multiferroic  \$\text{BiFeO}\_3\$  thin films epitaxially grown on  \$\text{SrRuO}\_3\$  bottom electrodes](#)

*Appl. Phys. Lett.* **108**, 112902112902 (2016); 10.1063/1.4944554

[Laser-assisted oxidation of multi-layer tungsten diselenide nanosheets](#)

*Appl. Phys. Lett.* **108**, 083112083112 (2016); 10.1063/1.4942802

[Properties of nanostructured undoped  \$\text{ZrO}\_2\$  thin film electrolytes by plasma enhanced atomic layer deposition for thin film solid oxide fuel cells](#)

*Appl. Phys. Lett.* **34**, 01A15101A151 (2015); 10.1116/1.4938105

[Microscopic thin film optical anisotropy imaging at the solid-liquid interface](#)

*Appl. Phys. Lett.* **87**, 043701043701 (2016); 10.1063/1.4947258

---



# Domain wall orientation and domain shape in $\text{KTiOPO}_4$ crystals

V. Ya. Shur,<sup>1,2,a)</sup> E. M. Vaskina,<sup>1</sup> E. V. Pelegova,<sup>1</sup> M. A. Chuvakova,<sup>1</sup>  
 A. R. Akhmatkhanov,<sup>1,2</sup> O. V. Kizko,<sup>3</sup> M. Ivanov,<sup>4</sup> and A. L. Kholkin<sup>1,4</sup>

<sup>1</sup>*Institute of Natural Sciences, Ural Federal University, 620000 Ekaterinburg, Russia*

<sup>2</sup>*Labfer Ltd., 620014 Ekaterinburg, Russia*

<sup>3</sup>*Crystals of Siberia Ltd., 630058 Novosibirsk, Russia*

<sup>4</sup>*Department of Physics and CICECO Aveiro Institute of Materials, 3810 193 Aveiro, Portugal*

(Received 10 June 2016; accepted 16 September 2016; published online 28 September 2016)

Domain shape evolution and domain wall motion have been studied in  $\text{KTiOPO}_4$  (KTP) ferroelectric single crystals using complementary experimental methods. The *in situ* visualization of domain kinetics has allowed revealing: (1) qualitative change of the domain shape, (2) dependence of the domain wall velocity on its orientation, (3) jump-like domain wall motion caused by domain merging, (4) effect of domain shape stability. The model of domain wall motion driven by generation of elementary steps (kink-pair nucleation) and subsequent kink motion is presented. The decrease in the relative velocity of the approaching parallel domain walls is attributed to electrostatic interaction. The effect of polarization reversal induced by chemical etching is observed. The obtained results are important for the development of domain engineering in the crystals of KTP family. *Published by AIP Publishing.* [<http://dx.doi.org/10.1063/1.4963781>]

Single crystals of potassium titanyl phosphate ( $\text{KTiOPO}_4$ , KTP) with periodical ferroelectric domain structures are widely used for nonlinear optical applications including forward and backward second harmonic generation<sup>1–4</sup> and optical parametric oscillation.<sup>5–8</sup> Moreover, the bulk periodically poled KTP single crystals with submicron periods were produced for realization of mirrorless optical parametric oscillation and backward second harmonic generation.<sup>9,10</sup> Deeper studies of the domain structure kinetics in KTP crystals are therefore necessary for further development of the periodical poling procedure of this material.

Domain structure kinetics during the polarization reversal can be considered as an analogue of the first order phase transition.<sup>11,12</sup> In this case, the local value of the electric field produced by various charge subsystems is the driving force for the nucleation process. The domain wall moves driven by generation of the elementary steps on it (kink-pair nucleation) and subsequent kink motion.<sup>13,14</sup> From this point of view, the domain structure evolution in KTP can be considered as a model process for investigation of the kinetics of the first order phase transitions in the crystals of  $C_{2v}$  symmetry.

Despite the great interest to the domain structure evolution in KTP, the *in situ* methods of domain visualization were much less used as compared with the crystals of lithium niobate and lithium tantalate family.<sup>15–18</sup>

Both integral and local methods can be used for *in situ* analysis of domain structure evolution during polarization reversal. The integral methods which allowed to obtain the information about the domain structure as a whole are applied for analysis of the homogeneity of periodically poled structure and for determination of the optimal poling time.<sup>19–21</sup> The local methods based on direct domain visualization provide the information about wall motion and shape evolution of the growing domains and allow to extract all

geometrical parameters of the domain structure.<sup>22,23</sup> Such methods are essential for deep understanding of the domain structure evolution which is crucial for the development of the physical basis of domain engineering in the crystals of  $C_{2v}$  symmetry.

The integral methods based on the electro-optic effect<sup>19</sup> and second harmonic generation in reflecting<sup>20</sup> and transmitting modes<sup>21</sup> were applied for the investigation of the periodical poling by inhomogeneous electric field in pure and doped KTP crystals.

Visualization of the domain evolution during the periodical poling of KTP by taking advantage of the electro-optic effect and a high speed camera was demonstrated by Hellstrom *et al.*<sup>22</sup> Application of the inhomogeneous electric field by stripe electrodes leads to formation of the periodic domain pattern. The *in situ* study of the domain structure evolution in uniform field was realized by Canalias *et al.*<sup>23</sup> only using quite challenging experimental method of digital holography. The obtained domain contrast was attributed to the phase difference appeared between light waves passing through the domains with opposite directions of the spontaneous polarization under an application of the uniform external electric field. The domain wall velocities along various crystallographic directions were estimated.<sup>23</sup> However, the problem of the method implementation resulted in studying domain kinetics in the narrow field range only. Moreover, the switching time about tens of milliseconds hampered the detailed investigation of the domain structure evolution.<sup>23</sup>

In this paper, we present results of *in situ* optical observation of the domain structure evolution in KTP single crystals in uniform electric field, which allowed us revealing the rhombus domain shape and the main domain wall orientations.

The studied KTP single crystals (Crystals of Siberia Ltd., Russia) were grown by top-seeded solution method. The bulk electrical conductivity at room temperature was about  $3 \times 10^{-9} \Omega^{-1} \text{cm}^{-1}$ . It has been previously noted that electrical conductivity of KTP decreases with the increasing

<sup>a)</sup> Author to whom correspondence should be addressed. Electronic mail: [vladimir.shur@urfu.ru](mailto:vladimir.shur@urfu.ru).

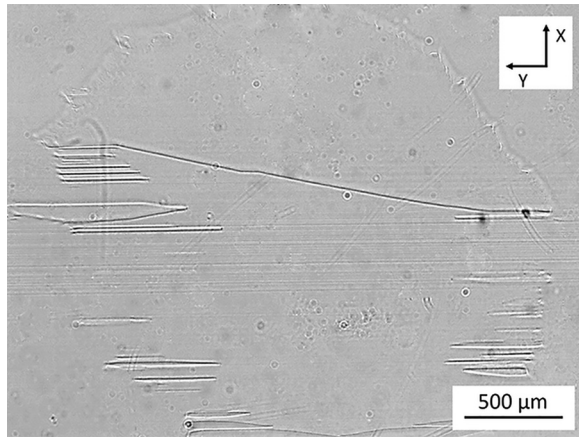


FIG. 1. Optical image of the domain pattern after partial polarization reversal using liquid electrodes without chemical etching. The contrast of domain walls is revealed only. Switching pulse parameters:  $E_{ex}$  3 kV/mm,  $t_p$  6.5 s.

potassium content.<sup>19</sup> According to the measured conductivity value, the potassium content in the studied sample lies between high and intermediate values.<sup>24</sup>

The studied samples represented 2-mm-thick and  $11 \times 16 \text{ mm}^2$  area plates cut perpendicular to polar axis. Metal and liquid electrodes were used for polarization reversal. The 100-nm-thick 2-mm-in-diameter Cr electrodes on Z+ polar surface and solid layer on Z− polar surface were deposited by electron-beam evaporation. The 2-mm-in-diameter liquid electrodes of the saturated LiCl aqueous solution were formed in the sample Plexiglas fixture with silicone rubber pads.<sup>25,26</sup>

The selective chemical etching in water solution of KOH and  $\text{KNO}_3$  mixture (2:1 mole ratio) at 80°C during 5–15 min was used for visualization of the static domain structure by optical microscopy and atomic force microscopy (AFM).<sup>1,17,20</sup> Moreover, the static domain structure was visualized without etching by optical microscopy (Fig. 1) and piezoresponse force microscopy (PFM). The atomic force microscope Ntegra Aura (NT-MDT, Russia) with Pt coated cantilevers (Budget Sensors, Bulgaria) was used for both AFM and PFM measurements.

The domain structure evolution was *in situ* visualized by experimental setup based on optical microscope (Carl Zeiss, Germany). The domain wall contrast was obtained for incoherent polarized light passed through the sample in polar direction. The high resolution (1 MPix) digital video camera (Allied Vision Prosilica GX1050C, USA) with frame rate up to 100 fps was used. The voltage pulse was generated by multifunctional data acquisition board NI PCI-6251 (National Instruments, USA) and amplified by high voltage

amplifier TREK 20/20C (Trek Inc., USA). The single rectangular pulse was applied for polarization reversal with duration ( $t_p$ ) ranged from 1 to 15 s and field amplitude ( $E_{ex}$ ) ranged from 3 to 4 kV/mm. It should be noted that the single unipolar pulse is usually applied for conventional periodical poling.<sup>27–30</sup>

The static domain structure visualized without chemical etching after partial polarization reversal encloses the isolated stripe domains elongated in Y crystallographic direction. More complicated domain shapes appeared as a result of domain merging.

The domain walls were oriented: (1) strictly along Y axis (Y walls), (2) strictly along X axis (X walls), (3) with deviations from Y axis ( $Y_+$  walls), and (4) with deviations from X axis about 30° ( $X_{+30}$  walls) (Fig. 2). The domain walls with irregular steps (Fig. 2(c)), appeared usually at the electrode edge, consisted of the Y-oriented fragments and those deviated from X axis. The revealed distance between adjacent parallel stripe domains achieved 1 μm (Fig. 2(a)).

The *in situ* visualization of the domain structure evolution during polarization reversal allowed us revealing two shapes of the nucleated isolated domain: stripe or rhombus elongated in Y direction (Figs. 3(a)–3(c)). The sharp angle of the rhombus domains ranged from 5° to 15°.

Two types of the moving domain walls have been distinguished: (1) the walls of the rhombus domains deviated from Y axis at the angle below 10° ( $Y_+$  walls), and (2) the walls deviated from X axis at the angle close to 30° ( $X_{+30}$  walls) (Figs. 3(b)–3(e)). The  $X_{+30}$  walls were essentially faster than  $Y_+$  walls.

The interaction of approaching  $Y_+$  domain walls led to formation of the stripe domain structures with short periods caused by decreasing of wall deviation from Y axis and motion deceleration (Fig. 2(a)).

The motion velocity of the  $X_{+30}$  domain walls increased from 0.2 mm/s at 3 kV/mm to 1.5 mm/s at 3.7 kV/mm, while the motion velocity of  $Y_+$  walls never exceeded 0.05 mm/s in the whole field range. It has been shown that the visible motion of  $Y_+$  walls is a result of merging of neighboring domains leading to the formation of the  $X_{+30}$  wall fragment, which moved rapidly along the  $Y_+$  wall (Fig. 4).

The concave angle formed during merging of  $X_{+30}$  walls disappeared within the time interval below the temporal resolution of our experimental setup (Fig. 5). The estimated wall motion velocity achieved 10 mm/s for external field 3 kV/mm. In this case, the distinguished wall trace was observed optically at the place of the previous wall position during the time interval about 0.1 s. The measured relaxation time of the wall trace was about 20 ms. It is necessary to

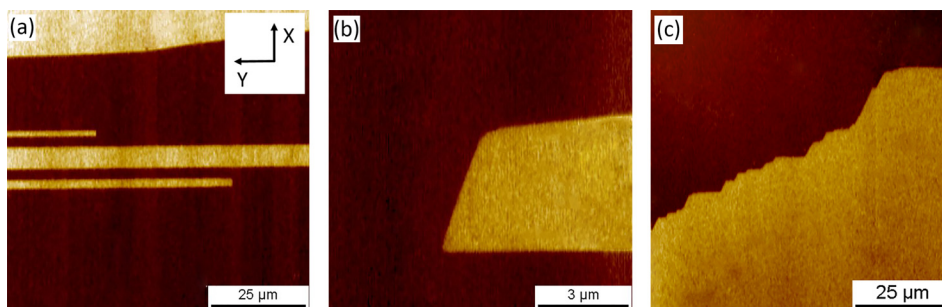


FIG. 2. The PFM images of the domain structure with different domain walls orientations. The switched domains correspond to bright areas.



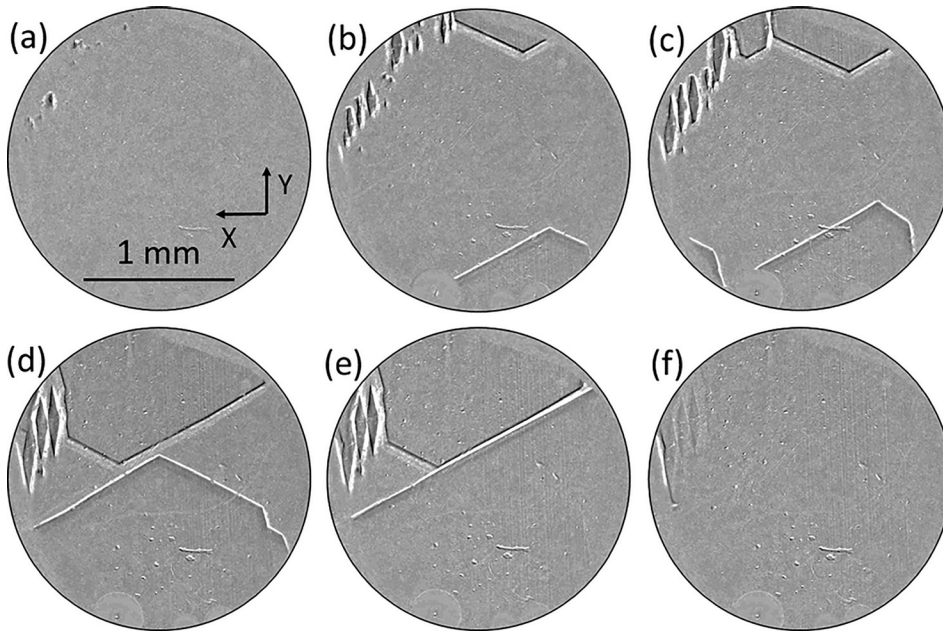


FIG. 3. The frames of domain structure kinetics during polarization reversal for  $E_{ex}$  3 kV/mm. Time for each frame: (a) 0.54 s, (b) 1.40 s, (c) 1.73 s, (d) 2.00 s, (e) 2.14 s, (f) 2.21 s.

point out that similar wall traces were observed during jump-like wall motion in lithium niobate crystals.<sup>31,32</sup>

The domain shape stability effect representing the restoration of the rhombus shape after merging of two small isolated rhombus domains has been revealed (Fig. 6). The formation of the  $X_{+30}$  domain wall was too fast to be resolved by used video camera (Fig. 6(c)). The fast motion of the appeared fragments of  $X_{+30}$  domain walls in opposite

Y directions (Figs. 6(c) and 6(d)) led to formation of large rhombus domain (Fig. 6(e)).

We have shown that the chemical etching leads to a change of the domain shape. The significant difference between PFM image of domain pattern and AFM image of etched relief (Fig. 7) is a clear demonstration of the etch-induced backswitching effect, which was discovered in doped stoichiometric lithium tantalate MgO:SLT.<sup>33</sup> Moreover, etching leads to an essential decrease of the wall deviation from Y axis and to the formation of X walls (Fig. 7). The backswitching has been attributed to the action of the polar component of low residual depolarization field ( $E_{rd}$ ) appeared as a result of partial removing of the screening charge by etching<sup>33</sup>

$$E_{rd} = E_{dep} - E_{scr}, \quad (1)$$

where  $E_{dep}$  is the depolarization field produced by bound charges and  $E_{scr}$  is the internal screening field.<sup>33</sup>

The demonstrated *in situ* optical visualization of the domain walls offers opportunities to study the domain structure evolution in KTP during polarization reversal. The obtained contrast of the domain walls is similar to results revealed earlier in the crystals of lithium niobate and lithium tantalate family.<sup>32,34–37</sup> The contrast can be attributed to local change of the refractive index in the vicinity of the domain wall under the action of transversal residual depolarization field due to the linear electrooptic effect.<sup>32,34,35</sup>

The appearance of the wall trace during jump-like domain wall motion in analogy with lithium niobate<sup>31,32,37,38</sup> can be attributed to retardation of the bulk screening, which leads to appearance of the transversal component of electric field in the region just passed by the fast domain wall.<sup>25</sup>

The *in situ* visualization of the domain structure evolution during polarization reversal allowed us to reveal the dominance of the relatively fast  $X_{+30}$  walls (Table I).

We propose to explain the observed wall orientations in terms of layer-by-layer growth model used for crystal growth.<sup>14</sup> We use the determined nucleation mechanism

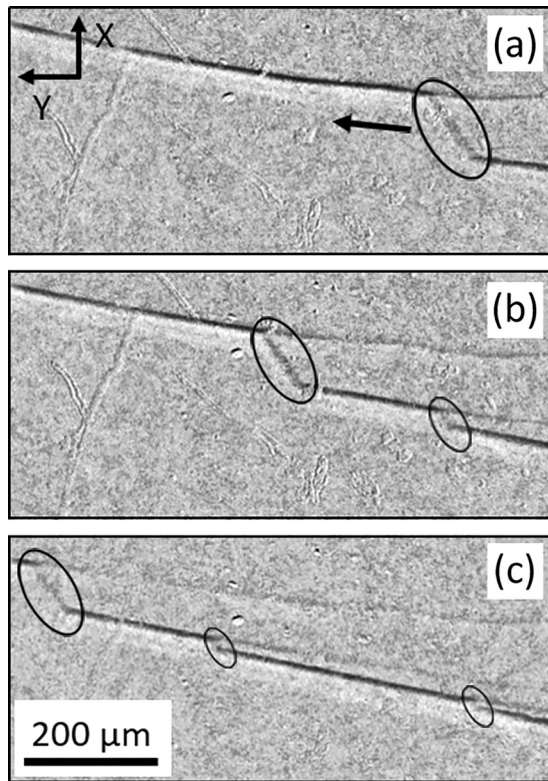


FIG. 4. Motion of  $X_{+30}$  wall fragments along  $Y_{+}$  domain wall. The fragments are encircled. The arrow at (a) indicates the direction of fragment motion. The time since the beginning of the switching process: (a) 2.0 s, (b) 2.4 s, (c) 2.8 s.  $E$  3 kV/mm.

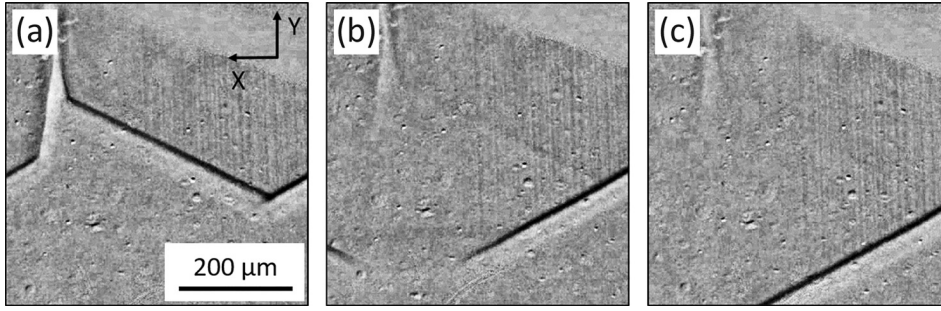


FIG. 5. Optical images demonstrating the jump like wall motion and formation of wall traces. The time since the start of the switching process: (a) 1.90 s, (b) 1.92 s, (c) 2.00 s.  $E = 3$  kV/mm.

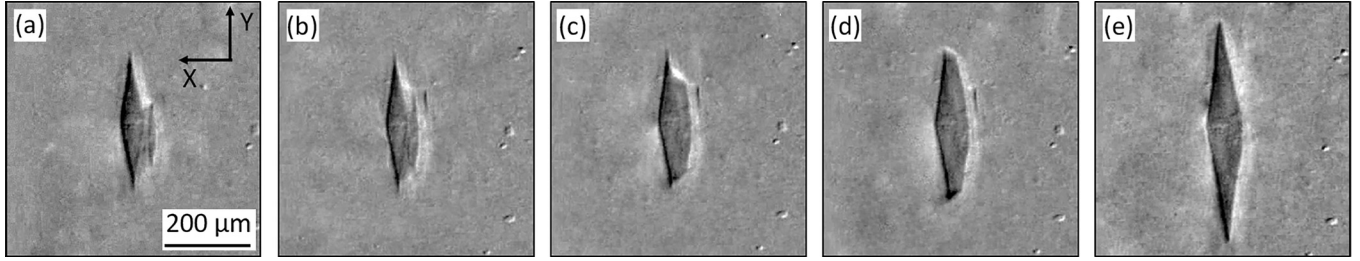


FIG. 6. Optical images demonstrating the shape stability effect. The time elapsed since the start of the switching process: (a) 1.40 s, (b) 1.63 s, (c) 1.65 s, (d) 1.70 s, and (e) 1.92 s.  $E = 3$  kV/mm.

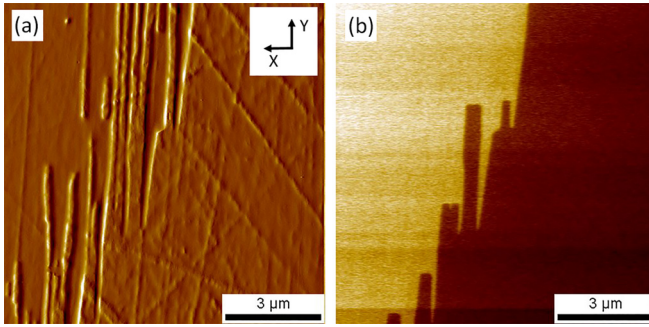


FIG. 7. (a) AFM image of etched relief, (b) PFM image of the domain pattern of the same place. Chemical etching after polarization reversal with metal electrodes.

with step generation at fixed nucleation sites at the polygon vertices of isolated domain, which have been discovered in lithium niobate crystals.<sup>32</sup> This mechanism leads to the formation of the vicinal walls, which deviation from the crystallographic axis and motion velocity is proportional to the kink density.

In such a case, the elementary steps are generated at the nucleation sites with subsequent kinks motion in  $Y$  directions (Fig. 8). As a result, the deviation of such “vicinal” wall from  $Y$  axis is defined by the kink density (Fig. 8(a)).

It is necessary to point out that the unit cell of KTP is elongated in  $X$ -direction; the lattice constants are:  $a = 12.819$  Å,  $b = 6.399$  Å,  $c = 10.584$  Å, where  $c$ -axis is the

polar direction.<sup>39</sup> According to the  $a/b$  ratio, the vicinal wall with maximal kink density is deviated from  $X$  axis at the angle  $26.5^\circ$  (Fig. 8(b)), which agreed with the experimentally observed orientation of  $X_{+30}$  wall. The stable vicinal walls can be clearly seen on PFM images obtained near the electrode edges (Fig. 2(c)).

It is clear that the wall motion velocity depends on the kink density. The  $X_{+30}$  walls with kink density about five times higher than that of typical  $Y_+$  walls moved about five times faster.

The revealed domain shape stability effect can be attributed to the formation of the fast  $X_{+30}$  wall after merging of rhombic domains and its fast motion until disappearance. As a result, the transition from two merged small rhombic domains to the single large one occurs within short time. The effect can be considered also as a consequence of the more general kinematic Wulff construction for crystal growth.<sup>14,40</sup>

The observed formation of the rectangular domains as a result of selective chemical etching can be attributed to polarization reversal in electric field being above the threshold value for kink motion, but below the one for step generation  $E_{th.s.gen} > E_{rd} > E_{th.s.gr}$ . In this case, the new kinks were not generated, while the existing ones moved till the domain edge. The diminishing of the wall deviation from the crystallographic axis caused by decrease of the kink density led finally to a transition from the vicinal walls to the singular  $Y$ - and  $X$ -oriented ones without any steps.

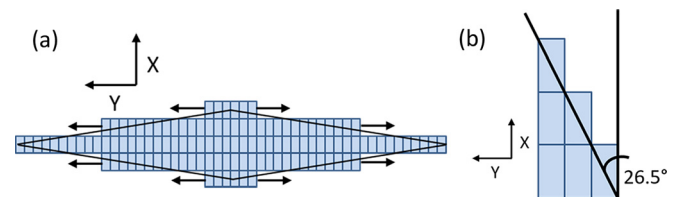


FIG. 8. The schematic of (a)  $Y_+$  walls of rhombus domain and (b)  $X_{+30}$  domain wall in KTP. Directions of kinks motion are marked by arrows.

TABLE I. Parameters of the moving domain walls revealed in KTP in the field 3 kV/mm.

Designation	Deviation from axis (deg)	Average motion velocity (mm/s)
$Y_+$	Below 10	Below 0.05
$X_{+30}$	About $30^\circ$	0.2



In conclusion, the domain shape evolution and kinetics of the domain structure were studied in KTP single crystals using complementary experimental methods. It was shown that the optical microscopy without selective chemical etching could be used for the visualization of domain wall statics and kinetics. This effect was related to the variation of the refractive index in the vicinity of the domain wall caused by residual depolarization field due to electrooptic effect. The *in situ* visualization of the domain structure evolution during polarization reversal allowed us to reveal two types of the isolated domain shapes: stripe and rhombus, oriented along Y direction. Two types of the moving domain walls were discerned. First, the walls of the rhombus domains deviated from Y-orientation for the angle below  $10^\circ$  ( $Y_+$  walls). Second, the walls deviated from X-orientation for the angle close to  $30^\circ$  ( $X_{+30}$  walls). It was shown that the  $X_{+30}$  walls were essentially faster than the  $Y_+$  ones. The motion velocities of both types of the walls were measured. The jump-like domain wall motion caused by domain merging was revealed. The domain shape stability effect representing the restoration of the rhombus shape after merging of small isolated rhombic domains was observed. The model of domain growth driven by generation of elementary steps and kink motion was proposed. The revealed effect of polarization reversal induced by chemical etching was attributed to the action of the low residual depolarization field appearing as a result of partial removing of the screening charge.

The equipment of the Ural Center for Shared Use “Modern Nanotechnology,” Ural Federal University was used. The research was made possible by Russian Foundation for Basic Research (Grant No. 16-02-00724-a). The work was supported by Government of the Russian Federation (act 211, agreement 02.A03.21.0006). V.Y.S. acknowledges financial support within the State Task from the Ministry of Education and Science of Russian Federation (Project No. 1366.2014/236). M.I. and A.L.K. acknowledge the CICECO-Aveiro Institute of Materials, POCI-01-0145-FEDER-007679 (Ref. FCT UID/CTM/50011/2013), financed by national funds through the FCT/MEC and when applicable co-financed by FEDER under the PT2020 Partnership Agreement.

<sup>1</sup>C. Canalias, V. Pasiskevicius, and F. Laurell, *Ferroelectrics* **340**, 27 (2006).

<sup>2</sup>X. Mu, I. B. Zotova, Y. J. Ding, and W. P. Risk, *Opt. Commun.* **181**, 153 (2000).

<sup>3</sup>X. Gu, M. Makarov, Y. J. Ding, J. B. Khurgin, and W. P. Risk, *Opt. Lett.* **24**, 127 (1999).

<sup>4</sup>A. Arie, G. Rosenman, V. Mahal, A. Skliar, M. Oron, M. Katz, and D. Eger, *Opt. Commun.* **142**, 265 (1997).

<sup>5</sup>D. Chuchumishev, G. Marchev, I. Buchvarov, V. Pasiskevicius, F. Laurell, and V. Petrov, *Laser Phys.* **10**, 115404 (2013).

<sup>6</sup>G. Marchev, P. Dallochio, F. Pirzio, A. Agnesi, G. Reali, V. Petrov, A. Tyazhev, V. Pasiskevicius, N. Thilmann, and F. Laurell, *Appl. Phys. B* **109**, 211 (2012).

<sup>7</sup>J. Hellstrom, V. Pasiskevicius, H. Karlsson, and F. Laurell, *Opt. Lett.* **25**, 174 (2000).

<sup>8</sup>A. Garashi, A. Arie, A. Skliar, and G. Rosenman, *Opt. Lett.* **23**, 1739 (1998).

<sup>9</sup>C. Canalias, V. Pasiskevicius, M. Fokine, and F. Laurell, *Appl. Phys. Lett.* **86**, 181105 (2005).

<sup>10</sup>C. Canalias and V. Pasiskevicius, *Nat. Photonics* **1**, 459 (2007).

<sup>11</sup>Y. Ishibashi and Y. Takagi, *J. Phys. Soc. Jpn.* **31**, 506 (1971).

<sup>12</sup>V. Shur, E. Romyantsev, and S. Makarov, *J. Appl. Phys.* **84**, 445 (1998).

<sup>13</sup>R. Miller and G. Weinreich, *Phys. Rev.* **117**, 1460 (1960).

<sup>14</sup>A. Pimpinelli and J. Villain, *Physics of Crystal Growth* (Cambridge University Press, Cambridge, 1998).

<sup>15</sup>V. Ya. Shur, E. V. Pelegova, A. R. Akhmatkhanov, and I. S. Baturin, *Ferroelectrics* **496**, 49 (2016).

<sup>16</sup>V. Ya. Shur and P. S. Zelenovskiy, *J. Appl. Phys.* **116**, 066802 (2014).

<sup>17</sup>E. Soergel, *Appl. Phys. B* **81**, 729 (2005).

<sup>18</sup>V. Ya. Shur, P. S. Zelenovskiy, M. S. Nebogatikov, D. O. Alikin, M. F. Sarmanova, A. V. Ievlev, E. A. Mingaliev, and D. K. Kuznetsov, *J. Appl. Phys.* **110**, 052013 (2011).

<sup>19</sup>H. Karlsson, F. Laurell, and L. K. Cheng, *Appl. Phys. Lett.* **74**, 1519 (1999).

<sup>20</sup>F. Laurell, M. G. Roelofs, W. Bindloss, H. Hsiung, A. Suna, and J. D. Bierlein, *J. Appl. Phys.* **71**, 4664 (1992).

<sup>21</sup>S. Wang, V. Pasiskevicius, and F. Laurell, *Opt. Mater.* **30**, 594 (2007).

<sup>22</sup>J. Hellstrom, R. Clemens, V. Pasiskevicius, H. Karlsson, and F. Laurell, *J. Appl. Phys.* **90**, 1489 (2001).

<sup>23</sup>C. Canalias, V. Pasiskevicius, F. Laurell, S. Grilli, P. Ferraro, and P. De Natale, *J. Appl. Phys.* **102**, 064105 (2007).

<sup>24</sup>G. Rosenman, P. Urenski, A. Arie, M. Roth, N. Angert, A. Skliar, and M. Tseitlin, *Appl. Phys. Lett.* **76**, 3798 (2000).

<sup>25</sup>V. Ya. Shur, A. R. Akhmatkhanov, I. S. Baturin, and E. V. Shishkina, *J. Appl. Phys.* **111**, 014101 (2012).

<sup>26</sup>V. Ya. Shur, A. R. Akhmatkhanov, M. A. Chuvakova, and I. S. Baturin, *Appl. Phys. Lett.* **105**, 152905 (2014).

<sup>27</sup>V. Ya. Shur, A. R. Akhmatkhanov, and I. S. Baturin, *Appl. Phys. Rev.* **2**, 040604 (2015).

<sup>28</sup>M. Yamada, N. Nada, M. Saitoh, and K. Watanabe, *Appl. Phys. Lett.* **62**, 435 (1993).

<sup>29</sup>L. E. Myers, R. C. Eckardt, M. M. Fejer, R. L. Byer, W. R. Bosenberg, and J. W. Pierce, *J. Opt. Soc. Am. B* **12**, 2102 (1995).

<sup>30</sup>G. W. Ross, M. Pollnau, P. G. R. Smith, W. A. Clarkson, P. E. Britton, and D. C. Hanna, *Opt. Lett.* **23**, 171 (1998).

<sup>31</sup>V. Ya. Shur, A. R. Akhmatkhanov, I. S. Baturin, M. S. Nebogatikov, and M. A. Dolbilov, *Phys. Solid State* **52**, 2147 (2010).

<sup>32</sup>V. Ya. Shur, *J. Mater. Sci.* **41**, 199 (2006).

<sup>33</sup>V. Ya. Shur, A. I. Lobov, A. G. Shur, S. Kurimura, Y. Nomura, K. Terabe, X. Y. Liu, and K. Kitamura, *Appl. Phys. Lett.* **87**, 022905 (2005).

<sup>34</sup>N. E. Yu and J. H. Ro, *Phase Transitions* **84**, 821 (2011).

<sup>35</sup>M. Muller, E. Soergel, and K. Buse, *Opt. Lett.* **28**, 2515 (2003).

<sup>36</sup>S. Kim and V. Gopalan, *Mater. Sci. Eng., B* **120**, 91 (2005).

<sup>37</sup>V. Gopalan, Q. X. Jia, and T. E. Mitchell, *Appl. Phys. Lett.* **75**, 2482 (1999).

<sup>38</sup>V. Gopalan and T. E. Mitchell, *J. Appl. Phys.* **85**, 2304 (1999).

<sup>39</sup>P. A. Thomas, A. M. Glazer, and B. E. Watts, *Acta Crystallogr., Sect. B: Struct. Sci.* **46**, 333 (1990).

<sup>40</sup>K. Romanyuk, V. Cherepanov, and B. Voigtlander, *Phys. Rev. Lett.* **99**, 126103 (2007).